# Longitudinal Assessment of Intraretinal Microvascular Abnormalities in Diabetic Retinopathy Using Swept-Source Optical Coherence Tomography Angiography

Xinyi Ding,[1] Francesco Romano,[1,2] Itika Garg,[1,3] Jenny Gan,[1] Katherine M. Overbey,[1] Mauricio D. Garcia,[1] Filippos Vingopoulos,[1,4] Ying Cui,[1] Ying Zhu,[1] Grace Baldwin,[1] Hanna Choi,[1] Jocelyn M. Rodriguez,[1] Matthew J. Finn,[1] Peyman Razavi,[1] Demetrios G. Vavvas,[2] Deeba Husain,[2] David M. Wu,[2] Nimesh A. Patel,[2] Leo A. Kim,[2] Joan W. Miller,[2] and John B. Miller[1,2]

[1]Harvard Retinal Imaging Lab, Department of Ophthalmology, Massachusetts Eye and Ear, Harvard Medical School, Boston, Massachusetts, United States
[2]Retina Service, Department of Ophthalmology, Massachusetts Eye and Ear, Harvard Medical School, Boston, Massachusetts, United States
[3]Department of Ophthalmology, Tulane University School of Medicine, New Orleans, Louisiana, United States
[4]Byers Eye Institute, Department of Ophthalmology, Stanford University School of Medicine, Palo Alto, California, United States

Correspondence: John B. Miller, Retina Service, Massachusetts Eye and Ear Infirmary, Harvard Medical School, 243 Charles St., Boston, MA 02114, USA; john_miller@meei.harvard.edu.

XD and FR contributed equally to this work.

**Received:** March 15, 2024
**Accepted:** June 29, 2024
**Published:** July 18, 2024

Citation: Ding X, Romano F, Garg I, et al. Longitudinal assessment of intraretinal microvascular abnormalities in diabetic retinopathy using swept-source optical coherence tomography angiography. *Invest Ophthalmol Vis Sci.* 2024;65(8):29. https://doi.org/10.1167/iovs.65.8.29

**Purpose.** To longitudinally investigate the changes in intraretinal microvascular abnormalities (IRMAs) over time, employing swept-source optical coherence tomography angiography in eyes with diabetic retinopathy.

**Methods.** In this retrospective, longitudinal study, we evaluated 12 × 12-mm swept-source optical coherence tomography angiography centered on the macula at baseline and last available follow-up visit for (1) IRMA changes during follow-up, defined as (a) stable, (b) regressed, (c) obliterated, and (d) progressed; and the (2) development of new neovascularization (NV) and their origins. Competing-risk survival analysis was used to assess the factors associated with these changes.

**Results.** In total, 195 eyes from 131 participants with diabetic retinopathy were included. Stable, regressed, obliterated, and progressed IRMA were observed in 65.1%, 12.8%, 11.3%, and 19% of eyes with diabetic retinopathy, respectively. Anti-VEGF injections during the follow-up periods and a slower increase of foveal avascular zone were associated with IRMA regression ($P < 0.001$ and $P = 0.039$). Obliterated IRMA were correlated with previous panretinal photocoagulation ($P < 0.001$) and a lower deep capillary plexus vessel density at baseline ($P = 0.007$), as well as with follow-up anti-VEGF injections ($P = 0.025$). A higher baseline ischemia index (ISI) and panretinal photocoagulation during the follow-up periods were associated with IRMA progression ($P = 0.049$ and $P < 0.001$). A faster increase in ISI predicted the development of NV elsewhere (NVE) from veins ($P < 0.001$). No significant factors were found to be associated with NVE originating from IRMA.

**Conclusions.** Changes in IRMA closely correlated with the severity of retinal ischemia and treatment. Notably, our study confirmed the potential, yet relatively rare, development of NVE from IRMA in a large cohort; however, the risk factors associated with this transformation require further exploration.

Keywords: intraretinal microvascular abnormalities, diabetic retinopathy, swept source OCT angiography

Intraretinal microvascular abnormalities (IRMA) were originally introduced in diabetic retinopathy (DR) classifications by Airlie House in 1968, without a clear definition whether this vascular abnormality represented new intraretinal blood vessel formation or dilation of preexisting capillaries.[1] Then subsequently Early Treatment of Diabetic Retinopathy Study standardized the assessment of IRMA, which were defined as tortuous intraretinal vascular segments located in standard fields 3 through 7, with caliber ranging from barely visible to 31 µm based on color

stereoscopic photograph.[2,3] As a result of these advancements, IRMA have gained significant importance as clinical biomarkers in the assessment of patients with DR. Development of IRMA has been proven to be associated with worsening severity of DR.[4] According to the International Clinical Diabetic Retinopathy Disease Severity Scale, the identification of prominent IRMA in one or more quadrants is sufficient to make a diagnosis of severe nonproliferative DR (NPDR).[5] Furthermore, in cases of severe NPDR, the presence of IRMA significantly increases the likelihood of progression to PDR, compared with cases with venous beading.[6]

Owing to the recent progress in retinal imaging, our understanding of IRMA has deepened as well. Color fundus photography (CFP) could only recognize prominent IRMA and faced challenges in effectively distinguishing these alterations from neovascularization (NV), a critical distinction for DR staging and management. Fluorescein angiography (FA) frequently serves as the distinguishing factor from NV as IRMA exhibit no or minimal leakage[7]; however, this imaging modality is both invasive and time-consuming. Optical coherence tomography (OCT) is a valuable technology that can provide more accurate anatomic insights than clinical examination or FA for comparing IRMA with NV.[7,8] OCT angiography (OCTA) is a noninvasive method to visualize the microvasculature in a depth-resolved manner, aiding in the distinction of IRMA from NV in DR.[9–16] Moreover, OCTA was reported to detect 50% of IRMA cases that were missed on CFP images.[12]

Studies using OCTA have described the morphological characteristics of IRMA, as well as their changes after treatment, including panretinal photocoagulation (PRP) and anti-VEGF injections.[10,14,17] Furthermore, some studies using longitudinal OCTA scanning have suggested the possibility of IRMA evolving directly into NV.[18] However, these studies have relatively small sample sizes, short follow-up duration, and a limited field of view. Therefore, the objective of this study is to employ expended field swept-source OCTA (SS-OCTA) in a large cohort of eyes with DR to characterize comprehensively changes in IRMA over time, investigate IRMA propensity to evolve into NV, and determine the predicting factors for these longitudinal IRMA changes.

## Methods

### Study Design and Subjects

This retrospective, longitudinal study was conducted at Massachusetts Eye and Ear Institute from December 2018 to March 2023. The study was approved by the Institutional Review Board of Massachusetts General Brigham (2019P001863), and informed consent was obtained from all participants. All procedures adhered to the tenets of the Declaration of Helsinki and Health Insurance Portability and Accountability Act regulations.

We included (1) adult patients aged >18 years diagnosed with type 1 or type 2 diabetes mellitus with (2) NPDR or PDR in one or both eyes, (3) a visual acuity of at least 20/200 Snellen, and (4) a minimum of 3 months of follow-up. Exclusion criteria included (1) inadequate image quality, defined as signal strength index less than seven or presence of significant artifacts, or (2) presence of other ocular comorbidities that might have affected our analysis, such as, coexisting retinal diseases other than hypertensive retinopathy and glaucoma other than neovascular cases.

### Procedures and Data Collection

All participants underwent comprehensive ophthalmic examinations at baseline and during follow-up visits, including medical history taking, visual acuity testing, slit-lamp examination, IOP measurement, macular OCT volume scans (Spectralis HRA+OCT2; Heidelberg Engineering GmbH, Heidelberg, Germany), ultra-widefield CFP (California, Optos plc., Dunfermline, UK) and dilated fundus

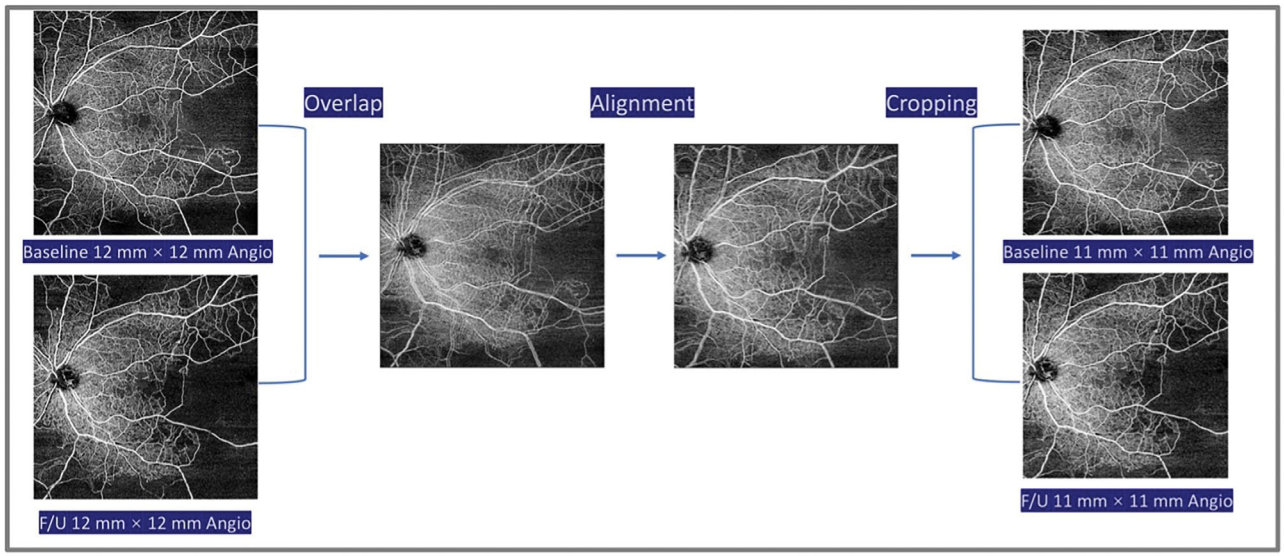


Figure 1. Flowchart of image trimming steps for image analysis using Adobe Photoshop. The OCTA images were obtained at baseline and the last available follow-up visit. First, one of the acquired images is overlaid with 50% opacity. Second, the image deviation is corrected by referencing the course of blood vessels. Finally, the opacity is restored to 100%, and the overlapping regions are cropped to 11 mm × 11 mm. F/U, follow-ups.

Investigative Ophthalmology & Visual Science

examination. Participants were then imaged using a 100-kHz SS-OCTA instrument (Plex Elite 9000, Carl Zeiss Meditec Inc., Dublin, CA) that uses a laser at a central wavelength of 1060 nm with a bandwidth of 100 nm. Angiography 12 × 12-mm scans centered on the macula were performed. Retinal vascular plexuses were segmented automatically by using the built-in custom segmentation of the device, with manual segmentation being allowed in case of segmentation error. FA could be performed at any timepoint during the follow-up at clinician's discretion. DR grading was initially collected from chart diagnoses performed by experienced senior retina specialists (J.B.M., D.G.V., D.H., N.A.P., J.W.M., D.M.W., and L.A.K.), based on clinical findings in accordance with the International Clinical Diabetic Retinopathy Disease Severity Scale.[5] These diagnoses were independently confirmed by a grader (X.D.) using ultra-widefield CFP, also adhering to International Clinical Diabetic Retinopathy Disease Severity Scale standards. Discrepancies between chart diagnoses and using ultra-widefield CFP observations were detected in 20 of 195 eyes, resulting in a 10.2% discrepancy rate. These discrepancies were resolved by our second grader (F.R.).

A comprehensive set of demographic and clinical data were collected from electronic medical records at baseline and during follow-up, including age, sex, smoking status (categorized as never, former, or current), type and duration of diabetes, glycated hemoglobin, insulin use, body mass index (BMI), hypertension, mean arterial blood pressure, visual acuity, IOP, lens status, ocular comorbidity, prior or current treatment (focal laser, PRP, anti-VEGF injection, and pars plana vitrectomy).

## Image Processing and Analysis

We evaluated 12 × 12-mm OCTA images from baseline and last available follow-up that met the OCTA image quality criteria by two independent masked ophthalmologists (X.D. and F.R.). A third grader (J.B.M.) adjudicated all cases of discrepancy.

For each 12 × 12-mm scan, the presence of the following abnormalities were qualitatively assessed based on their characteristics on en face OCTA images and the corresponding OCT volume: diabetic macular edema, IRMA (tortuous, dilated, and looped intraretinal new vessels adjacent to the areas of capillary loss), NV (extraretinal hyperreflective lesions contiguous within a single B-scan or range of B-scans), NV of the optic disc (NVD, defined as NV located in the optic disc or within 1 disc diameter from the margin), NV elsewhere (NVE, defined as NV located beyond a range of 1 disc diameter from the disc margin), and nonperfusion

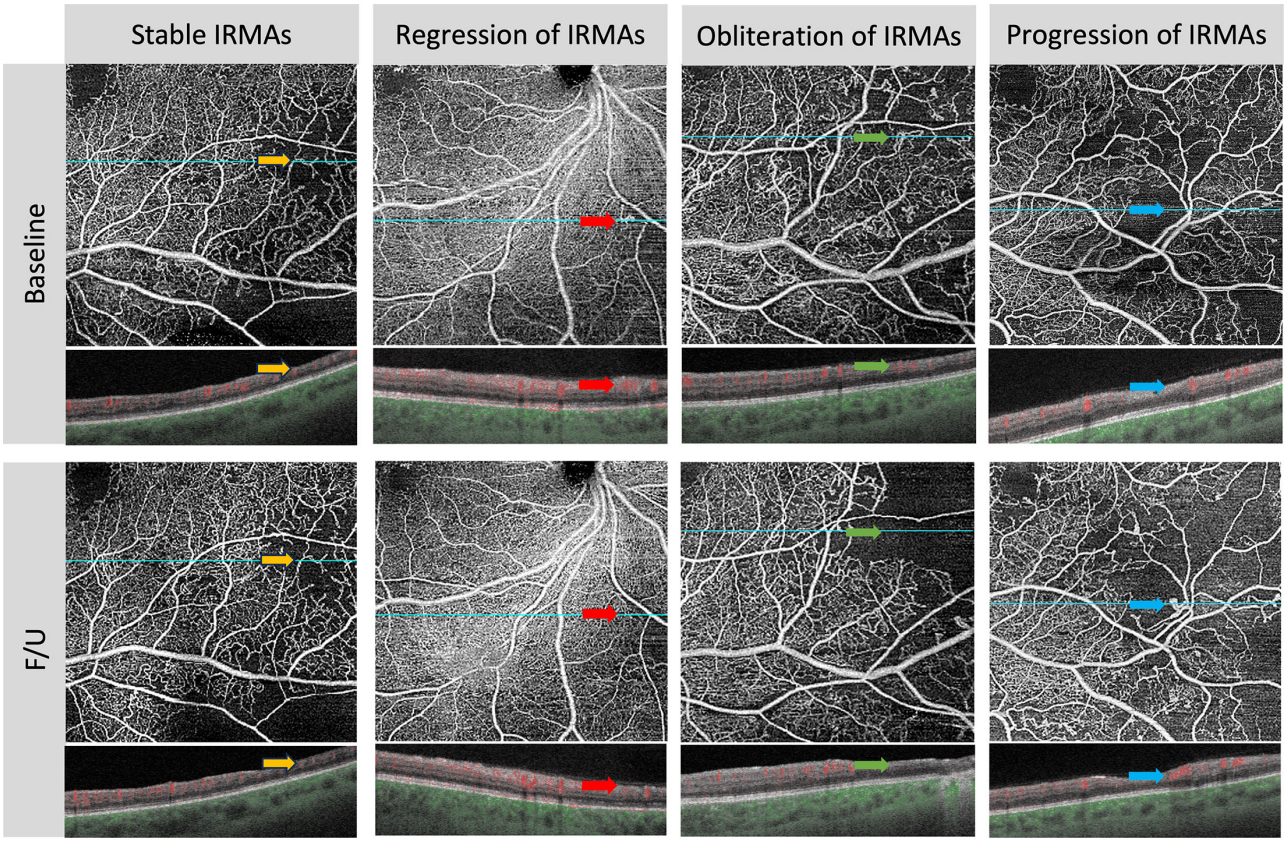


**Figure 2.** Four subtypes of morphological changes in the IRMAs. (1) Stable IRMA (*yellow arrow*). All IRMA lesions maintain their original structure, including branch count, vessel caliber, and the area of nonperfused tissue around them, without any changes. (2) Regression of IRMA (*red arrow*). At least one site of abnormal IRMA branches disappears or gradually integrates with the nearby normal capillary bed, resembling the typical pattern of healthy blood vessels (reperfusion). This occurs without an expansion of the surrounding NPA. (3) Obliteration of IRMA (*green arrow*). In at least one location, the IRMA structures begin to vanish, corresponding to the progression of nonperfused areas in the capillary bed. (4) Progression of IRMA (*blue arrow*). In at least one location, there is an increase in the branching of the abnormal IRMA blood vessels, accompanied by the possible emergence of new IRMA structures, sometimes with nonperfused areas around them increases. F/U, follow-ups.

Investigative Ophthalmology & Visual Science

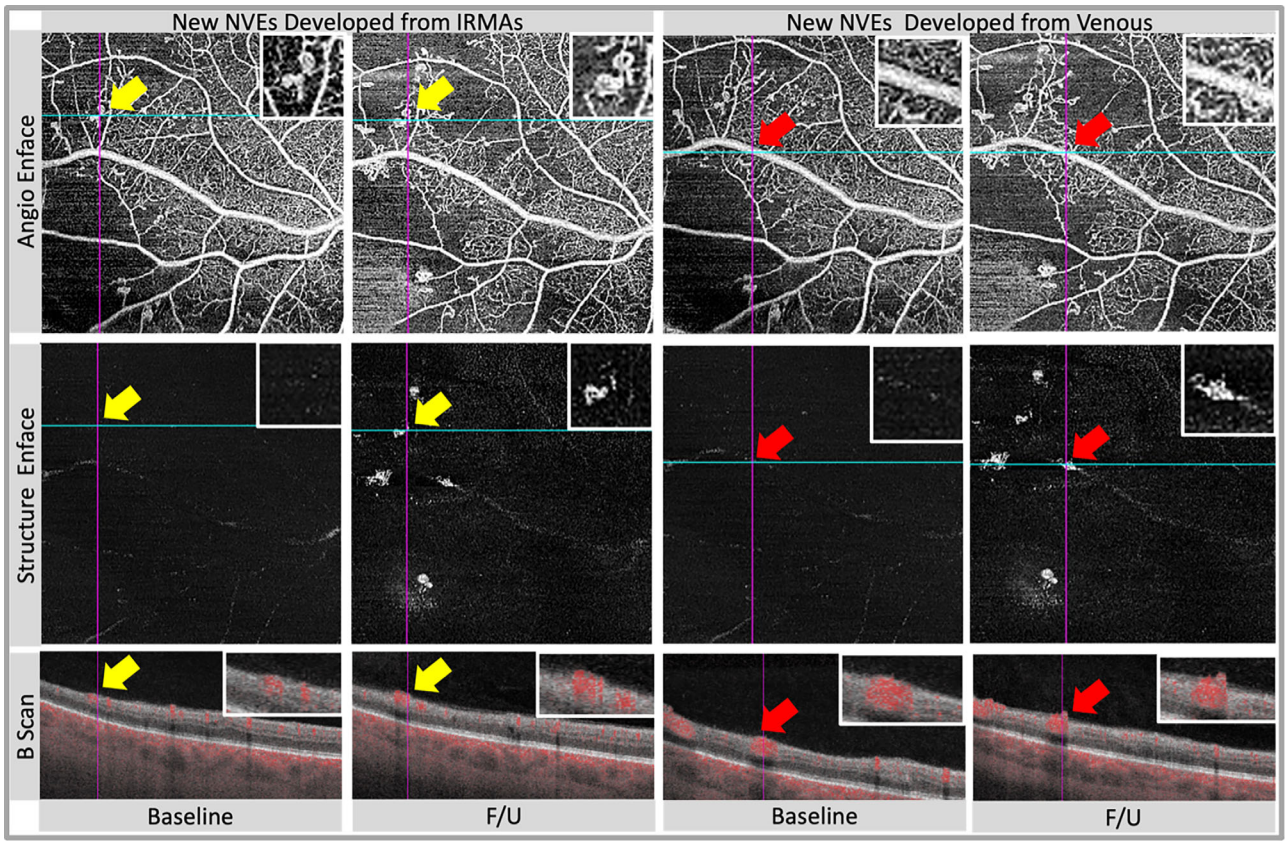


**Figure 3.** Examples of neovascularizations elsewhere (NVEs) from different sources. The sources of NVE can be categorized into the following two types. In (1) NVE originating from IRMAs (*yellow arrow*), the precursor lesions of IRMA initially present as intraretinal tortuous vascular abnormalities without breaching the inner limiting membrane (ILM), subsequently progressing into preretinal NV that breaches the ILM. In (2) NVE originating from venules (*red arrow*), neovascularizations centered around venules, with stems originating from venules with blood flow signals. F/U, follow-ups.

areas (NPAs, defined as regions of capillary loss equal to or exceeding one-fourth of the optic disc's area).[19] Breaching of the inner limiting membrane served as a critical anatomical landmark to distinguish NV from IRMA.

To obtain an accurate evaluation of the qualitative changes occurring in IRMA, NV, and NPA, baseline and last available follow-up 12 × 12-mm angiographic images and structure enface images were imported into Photoshop (Adobe, San Jose, CA, USA). The follow-up scan was overlaid using 50% opacity and then the image deviation was corrected by referencing the course of blood vessels. Finally, opacity was restored to 100%, and the overlapping regions were cropped to 11 × 11-mm to account for the minimal differences in foveal centration (Fig. 1).

The presence and morphological changes of IRMA were examined on superficial and full-thickness retina slabs in the cropped angiograms.[14,17] We categorized the morphological changes in IRMA into four subtypes (Fig. 2) according to previous literature[14,17]: (1) stable, all IRMA lesions maintain their original structure, including branch count, vessel caliber, and the surrounding area of nonperfused tissue; (2) regression, at least one site of abnormal IRMA branches disappears or gradually integrates with the nearby normal capillary bed, resembling reperfusion and without an expansion of the surrounding NPA; (3) obliteration, IRMA structures begin to vanish in at least one location, corresponding with the progression of nonperfused areas in the capillary bed; and (4) progression, an increase in the branching of the abnormal IRMA blood vessels in at least one location, possibly accompanied by new IRMA structures and by an increase in the nonperfused areas around them. If multiple IRMA lesions within the scanning range manifested various changes, they were all recorded.

When evaluating the occurrence of new NVE during the follow-up, we recorded their source as follows (Fig. 3): (1) NVE originating from IRMA, which subsequently progressed into preretinal NV with continuous intraretinal components[11,18] and (2) NVE originating from retinal veins.[11,20] NPAs were measured using the superficial capillary plexus slabs of cropped 11 × 11-mm angiograms, based on a previously published semiautomated algorithm using ImageJ FIJI.[21] The ischemia index (ISI) was defined as area of nonperfusion divided by total area.

The following quantitative OCTA metrics were calculated using the Macular Density v0.7.3.3 software on the ARI Network (Zeiss Portal v5.4-1206): macular vessel density (defined as the ratio of the covered vessel area divided by the total area of a region of interest) and vessel skeletonized density (VSD, defined as the ratio of the cumulative length of all vessels in a region of interest divided by the area of the region of interest) on the superficial capillary plexus, deep capillary plexus (DCP), and full-thickness retina slabs for 12 × 12-mm scans, foveal avascular zone (FAZ) metrics (FAZ area, circularity, and perimeter) on the superficial reti-

Investigative Ophthalmology & Visual Science

nal layer for 12 × 12-mm scans. The algorithm used legacy segmentation to define the superficial and deep slabs.

Changes in systemic, ocular, and OCTA metrics over time were defined as the difference between the last and first examination divided by time.

### Statistical Analysis

Statistical analysis was performed using Stata version 18.0 (StataCorp; College Station, TX, USA). Descriptive statistics were reported as median, accompanied by the first and third quartiles or frequency (percentage) as appropriate. The repeatability between graders for qualitative measures was assessed using the Cohen's k-factor. Changes in OCTA metrics over time were assessed using the Wilcoxon signed-rank test. All tests were two sided, and a $P$ value of $<0.05$ was considered statistically significant.

Baseline and time-varying demographic, clinical and OCTA parameters were all considered as predictors and tested by leveraging the least absolute shrinkage and selection operator regression for Cox mixed-effects models with IRMA changes and new NV as dependent variables. Age, duration of diabetes, and baseline glycated hemoglobin level were selected as constant inclusions in the models. The Bayesian information criterion was used to select a parsimonious model (e.g., fewer predictors), increasing model stability while accounting for data multicollinearity; moreover, 10-fold cross-validation was used to improved prediction accuracy.

Subsequently, the selected variables were integrated as fixed effects into multivariable competing-risk survival models to explore the predictors for (1) IRMA change over time (stable IRMA vs regression of IRMA, obliteration of IRMA and progression of IRMA) and (2) new NVE development (no new NVE vs. NVE from veins and NV from IRMA). Results were reported through hazard ratios (HR) with 95% confidence intervals (CIs) and $P$ values. All models were adjusted for age, glycated hemoglobin and diabetes duration at the baseline visit.

## Results

### Demographics and Ocular Characteristics of Participants

For this study, 693 eyes with NPDR and 607 eyes with PDR have been reviewed, and 71 eyes were excluded owing to the presence of ocular comorbidities. Additionally, 1024 eyes were excluded for inadequate image quality during baseline or follow-up visits, or for having <3 months of follow-up time.

Overall, 98 eyes from 63 patients with NPDR (32 eyes with mild NPDR, 49 eyes with moderate NPDR. and 17 eyes with severe NPDR) and 97 eyes from 68 patients with PDR were included. Patients in the NPDR group had a median age of 62.0 years (interquartile range [IQR], 52.3–68.0 years), whereas those in the PDR group were 57.0 years of age (IQR, 47.5–63.0 years). The median diabetes duration was 13.5 years (IQR, 7.0–23.0 years) for NPDR and 22.0 years (IQR, 14.3–30.0 years) for PDR group, with 50.8% of patients in the NPDR group and 51.5% patients in the PDR group being female. The follow-up period using OCTA for the NPDR group ranges from 3.3 to 42.9 months with a median of 17.0 months (IQR, 12.0–27.0 months), whereas for the PDR group, it ranges from 3.2 to 46.6 months with a median of 15.0 months (IQR, 7.5–26.0 months). Demographic and systemic parameters, ocular characteristics of study participants in the cohort are presented in Tables 1 and 2.

**Table 1.** Demographic and Systemic Characteristics at Baseline

| | NPDR | PDR |
|---|---|---|
| No. of patients | 63 | 68 |
| Age, years | 62.0 (54.0–68.0) | 57.5 (47.5–63.0) |
| Gender (female) | 29 (46.0) | 25 (36.8) |
| Type of diabetes | | |
| T1DM | 10 (15.9) | 17 (25.0) |
| T2DM | 53 (84.1) | 46 (67.6) |
| Diabetes duration, years | 13.0 (7.0–23.0) | 22.0 (14.3–30.0) |
| BMI (kg/m$^2$), baseline | 32.2 (27.8–38.9) | 29.7 (24.6–34.8) |
| HbA1C (%), baseline | 7.9 (6.9–8.7) | 8.0 (7.2–9.2) |
| Insulin treatment, yes | 43 (68.3) | 54 (79.4) |
| Hypertension, yes | 49 (77.8) | 48 (70.6) |
| MABP, mm Hg | 95.3 (88.7–102.7) | 95.0 (88.7–104.3) |
| Smoking status* | | |
| Current | 3 (4.8) | 8 (11.8) |
| Former | 27 (42.9) | 12 (17.6) |
| Never | 31 (49.2) | 41 (60.3) |

F/U, follow-ups; HbA1c, glycated hemoglobin; MABP, mean arterial blood pressure; T1DM, type 1 diabetes mellitus; T2DM, type 2 diabetes mellitus.

Values are median (IQR) or number (%).

**Table 2.** Ocular Characteristics at Baseline and F/U

| | NPDR | PDR |
|---|---|---|
| No. of eyes | 98 | 97 |
| Laterality, OD | 48 (49.0) | 55 (56.7) |
| BCVA, Letters, baseline | 80 (74–84) | 78 (70–82) |
| IOP (mm Hg), baseline | 17.0 (14.0–19.0) | 17.0 (15.0–18.0) |
| DME, baseline, yes | 70 (71.4) | 59 (60.8) |
| Lens status | | |
| Phakia | 71 (72.4) | 58 (59.8) |
| Pseudophakia | 27 (27.6) | 39 (40.2) |
| Prior history of treatment | | |
| None | 71 (72.4) | 48 (49.5) |
| Injection | 26 (26.5) | 39 (40.2) |
| Focal laser | 3 (3.1) | 8 (8.2) |
| PRP | 0 | 12 (12.4) |
| PPV | 0 | 5 (5.2) |
| Treatment during F/U | | |
| None | 57 (57.2) | 42 (43.3) |
| Injection | 41 (41.8) | 47 (48.5) |
| Focal laser | 0 | 2 (2.1) |
| PRP | 2 (2.0) | 17 (17.5) |
| PPV | 0 | 0 |
| OCTA F/U time, months | 17.0 (12.0–27.0) | 15.0 (7.5–26.0) |

BCVA, best corrected visual acuity; DME, diabetic macular edema; F/U, follow-ups; PPV, pars plana vitrectomy.

Values are median (IQR) or number (%).

### WF SS-OCTA Findings

At the baseline visit, 52% of eyes in the NPDR group exhibited IRMA in the 12 × 12-mm angiography centered at the macula, whereas in the PDR group, this percentage was higher at 95%. NPA were present in 68% of eyes with NPDR and in all eyes with PDR (100%). During follow-up, the

Investigative Ophthalmology & Visual Science

proportion of eyes with NPDR with IRMA increased to 60.0% and with NPA to 74.5%. In the PDR group, the proportion of eyes with IRMA also increased to 98.9%.

Stability in IRMA was observed in 75.5% of eyes with NPDR and 54.6% of eyes with PDR. IRMA regression was noted in 8.2% of eyes with NPDR and 17.5% of eyes with PDR. Among eyes with NPDR, 5.1% exhibited IRMA obliteration, whereas this percentage was higher for eyes with PDR (17.5%). We found that 16.3% of eyes with NPDR and 21.6% of eyes with PDR experienced IRMA progression.

Over the follow-up period, 4.1% of eyes with NPDR and 18.6% of eyes with PDR displayed the emergence of new NV. In detail, 5.0% of eyes with NPDR and 15.5% of eyes with PDR demonstrated new NVE originating from venous sources. Development of new NVE from IRMA was observed in 7.2% of eyes with PDR, although this finding was not observed in the NPDR group. Furthermore, 3.1% of eyes with NPDR and 5.2% of eyes with PDR exhibited the appearance of new NVD.

The inter-rater reliabilities for the presence of IRMA, NPA, NVE, NVD, IRMA transformations, and NV development were moderate to good (Supplementary Table S1).

The ISI showed a significant increase during follow-up in both NPDR (from 0.03 [IQR, 0–0.07] to 0.04 [IQR, 0–0.09]; $P < 0.001$) and PDR (from 0.14 [IQR, 0.11–0.14] to 0.17 [IQR, 0.11–0.23]; $P < 0.001$) groups. In the NPDR group, both vessel density and VSD in the DCP slab decreased, with vessel density decreasing from 0.16 (IQR, 0.10–0.23) to 0.14 (IQR, 0.09–0.19) ($P = 0.552$), and the VSD decreasing from 5.93 (IQR, 3.86–8.73) to 4.91 (IQR, 3.11–6.81) ($P = 0.035$). In the PDR group, vessel density decreased significantly from 0.15 (IQR, 0.10–0.19) to 0.12 (IQR, 0.08–0.17) ($P = 0.001$), and VSD from 5.36 (IQR, 3.73–6.82) to 4.32 (IQR, 3.05–5.93) ($P = 0.001$). FAZ circularity was increased significantly over time ($P = 0.031$) in the NPDR group. WF SS-OCTA characteristics of study participants are outlined in Table 3 and Supplementary Table S2.

**Table 3.** WF SS-OCTA Characteristics at Baseline and F/U

| | NPDR | PDR |
|---|---|---|
| Baseline | | |
| IRMA, yes | 52 (53.1) | 95 (97.9) |
| NPA, yes | 68 (69.4) | 97 (100) |
| NVE, yes | 4 (4.1) | 68 (70.1) |
| NVD, yes | 1 (1.0) | 30 (30.9) |
| F/U | | |
| IRMA, yes | 60 (61.2) | 96 (99.0) |
| NPA, yes | 73 (74.5) | 97 (100) |
| NVE, yes | 6 (6.1) | 71 (73.2) |
| NVD, yes | 4 (4.1) | 33 (34.0) |
| IRMA changes during F/U | | |
| Stable, yes | 74 (75.5) | 53 (54.6) |
| Progression, yes | 16 (16.3) | 21 (21.6) |
| Regression, yes | 8 (8.2) | 17 (17.5) |
| Obliteration, yes | 5 (5.1) | 17 (17.5) |
| Both progression and obliteration, yes | 2 (2.0) | 4 (4.1) |
| Both regression and obliteration, yes | 0 | 1 (1.0) |
| Both regression and progression, yes | 3 (3.1) | 7 (7.2) |
| New NV development during F/U | | |
| Any new NV, yes | 4 (4.1) | 18 (18.6) |
| New NVE developed from venules, yes | 5 (5.0) | 15 (15.5) |
| New NVE developed from IRMA, yes | 0 | 7 (7.2) |
| New NVD, yes | 3 (3.1) | 5 (5.2) |

F/U, follow-ups; NV, neovascularizations; NVD, neovascularizations of the optic disc; NVE, neovascularizations elsewhere.

## Factors Associated With IRMA Changes

The multivariate mixed-effect Cox regression analysis revealed that no hypertension at baseline (HR, 0.30; 95% CI, 0.13–0.68; $P = 0.004$), along with anti-VEGF injection treatment during follow-up (HR, 3.33; 95% CI, 1.07–10.21; $P = 0.039$) and a slower FAZ increase (HR, 0.01; 95% CI, 0.00–0.26; $P = 0.007$), were associated with regression of IRMA.

**Table 4.** Baseline and Time-Varying Predictors for IRMA Changes and NV Development

| Outcomes | Baseline Characteristics | Hazard Ratio (HR) | 95% CI | *P* Value |
|---|---|---|---|---|
| Regression of IRMA | Hypertension | 0.30 | 0.13–0.68 | 0.004 |
| Obliteration of IRMA | Prior PRP | 13.57 | 15.33–1622.31 | <0.001 |
| | Vessel density DCP 12 mm × 12 mm angiography | 0.74 | 0.59–0.92 | 0.007 |
| Progression of IRMA | Ischemia index (ISI) | 23.17 | 1.01–529.95 | 0.049 |
| **Outcomes** | **Time-Varying Characteristics** | **Hazard Ratio (HR)** | **95% CI** | ***P* Value** |
| Regression of IRMA | FAZ | 0.01 | 0–0.26 | <0.001 |
| | Injection during F/U | 3.33 | 1.07–10.21 | 0.039 |
| Obliteration of IRMA | BMI | 4.19 | 2.49–7.04 | <0.001 |
| | F/U injection | 3.96 | 1.19–13.18 | 0.025 |
| Progression of IRMA | PRP during F/U | 5.30 | 2.08–13.5 | <0.001 |
| **Outcomes** | **Baseline Characteristics** | **Hazard Ratio (HR)** | **95% CI for HR** | ***P* Value** |
| NVE from vein | HbA1c | 1.117 | 1.011–1.235 | 0.030 |
| NVE from IRMA | N/A | | | |
| **Outcomes** | **Time-Varying Characteristics** | **Hazard Ratio (HR)** | **95% CI** | ***P* Value** |
| NVE from veins | ISI | 6.02 | 2.73–13.29 | <0.001 |
| NVE from IRMA | | N/A | | |

DME, diabetic macular edema; F/U, follow-ups; HbA1c, glycated hemoglobin; ISI, nonperfusion areas/total area; N/A, not available; NV, neovascularizations; NVD, neovascularizations of the optic disc; NVE, neovascularizations elsewhere; PRP, pan retinal photocoagulation.

Investigative Ophthalmology & Visual Science

For the obliteration of IRMA, significant baseline predictive factors included prior PRP (HR, 13.57; 95% CI, 15.33–1622.31; $P < 0.001$) and lower vessel density in the DCP slab of 12 × 12-mm angiography (HR, 0.74; 95% CI, 0.59–0.92; $P = 0.007$). Significant time-varying predictors included BMI increase (HR, 4.19; 95% CI, 2.49–7.04; $P = 0.006$) and anti-VEGF injection treatment during the follow-up periods (HR, 3.96; 95% CI, 1.19–13.18; $P = 0.025$).

For the progression of IRMA, a higher ISI at baseline and a PRP during the follow-up periods were identified as significant predictors with HRs of 23.17 (95% CI, 1.01–529.95; $P = 0.049$) and 5.30 (95% CI, 2.08–13.5; $P < 0.001$), respectively (Table 4).

### Factors Associated With the Occurrence of New NVE

A faster increase in the ISI during the follow-up periods was associated with NVE originating from veins, with HR of 6.02 (95% CI, 2.73–13.29; $P < 0.001$). No significant factors were found to be associated with NVE originating from IRMA.

## Discussion

The present study is the first to use expanded field SS-OCTA imaging for a comprehensive longitudinal evaluation of IRMA, tracking their potential progression to retinal NV, and identifying the predictive factors associated with these changes. No hypertension or anti-VEGF injections and a slower FAZ increase during follow-up were associated with their regression. In contrast, prior PRP, lower vessel density in the 12 × 12-mm DCP slab at baseline, anti-VEGF injection, and a faster increase of BMI during follow-up were associated with obliteration of IRMA. A higher ISI at baseline and PRP during the follow-up periods were identified as significant predictors for progression of IRMA. Progression of preexisting IRMA into new NV was observed in 7 of 92 eyes with PDR (7.2%). A faster increase in the ISI during follow-up was recognized as a notable predictor for the NV developed from veins. No significant factors were found to be associated with NVE originating from IRMA.

Although early detection and timely treatment can prevent most cases of vision loss and blindness, DR remains a leading cause of visual impairment in the working-age population worldwide, emphasizing the urgent need for enhanced screening and intervention strategies.[22] Advances in OCTA have enhanced IRMA detection rates, improved the efficiency of distinguishing IRMA and NV, and deepened our understanding of IRMA, which is one of the most vital microvascular features for DR grading.[9–16] Sorour et al.[14] graded IRMA changes for both anti-VEGF intervention and nonintervention scenarios, categorizing them as stable IRMA, regression of IRMA, obliteration of IRMA, and progression of IRMA. Based on this research, we applied these categories to expanded field (12 × 12-mm) SS-OCTA scans.

We indicated that anti-VEGF injections during follow-up serve as a predictive factor for IRMA regression. This observation corresponds with Sorour et al.'s study, where 14 of 45 IRMA lesions in the treated group regressed, and no regression was observed in the control group,[14] raising the question of whether the role of VEGF in IRMA is associated with promoting the development of NV. Additionally, we observed that a slower increase in the FAZ is an associated factor for IRMA regression. The FAZ, a specialized region of the retina, contains the greatest density of cone photoreceptors and exhibits high oxygen consumption.[23] Enlargement of the FAZ in patients with diabetes has been quantified using FFA and OCTA and associated with the severity of DR.[24,25] The slower progression of the FAZ may suggest a slowing of the worsening ischemia in the macular area. This finding is linked to the regression of IRMA and could indicate that the progression of the patient's DR is being effectively managed or that the treatment is yielding positive responses. No hypertension was found to be another factor associated with IRMA regression, a finding not indicated previously by other studies. However, several randomized controlled trials have demonstrated that uncontrolled hypertension can lead to the onset or progression of DR.[26,27]

Prior PRP and lower vessel density in the DCP of 12 × 12-mm angiography scans, along with anti-VEGF injections during follow-up, all suggest a more severe degree of retinal ischemia in the eyes. These factors have been linked to the obliteration of IRMA, suggesting that eyes with more severe ischemia may be more susceptible to NPA expanding and capillary drop-out over time. A faster increase in BMI was found to be correlated with the obliteration of IRMA. In previous studies, increased BMI has shown an inverse association with DR, yet it was positively associated with the progression of DR.[28–30] However, the correlation between changes in BMI over time and the progression of DR has not been described.

A higher ISI at baseline was associated with the onset and progression of IRMA. This finding is consistent with its underlying mechanisms, which involve either the growth of new vessels within the retina or the remodeling of existing vessels. This process is driven by endothelial cell proliferation, stimulated by hypoxia in areas bordering capillary nonperfusion.[2,31] PRP during the follow-up period was shown as another associated factor, which might be explained by the fact that patients requiring PRP treatment inherently have a more severe degree of DR or exhibit significant progression during the follow-up process.

Our study also confirms the potential progression of preexisting IRMA into new NV, observed in 7 of 97 eyes with PDR (7.2%). This progression was not only supported by the histological similarity and colocalization of IRMA and NV lesions,[31,32] but was also hypothesized through previous OCT, FA, and OCTA studies.[7,18] Additionally, Shimouchi et al.[17] found that tufts in IRMA, exhibiting characteristics that resemble NV, were more frequently observed in the eyes with PDR (15/20 [75%]) compared with eyes with severe NPDR. This might help to explain why IRMA progressing into NV were only observed in eyes with PDR and not in the NPDR group.

Interestingly, IRMA are not the sole source of NV: NVD are suggested to be originated from the retinal artery, the retinal vein, or the choroid,[11,33,34] whereas NVE are proposed to possibly arise from veins or IRMA. A faster increase in the ISI over time was identified as a significant risk factor for the development of NVE from veins, highlighting the role of ongoing ischemic progression in this process. However, no significant risk factors were identified for new NVE originating from IRMA. One possible explanation could be the low incidence of these events—only 7 of 195—which may not provide sufficient statistical power to detect significant risk factors.

Investigative Ophthalmology & Visual Science

This study has several limitations. First, owing to its retrospective and longitudinal nature, standardized follow-up times were not established. To mitigate selection bias stemming from varying imaging frequencies during follow-up, we chose the last OCTA scan during the follow-up that met the OCTA image quality standards for analysis. Additionally, we incorporated the interval between this final OCTA follow-up and the baseline into our survival analysis. In future follow-ups, we plan to collect key time points, such as 6 months, 12 months, and 24 months, and conduct consecutive studies on IRMA transformation. Another limitation is that the prior treatments received by some participants, which impeded a precise evaluation of IRMA's pretreatment condition and its inherent progression. Furthermore, although we considered the anti-VEGF treatment received prior to and during the follow-up periods as predictive factors, we did not take into account the number of anti-VEGF injections or the time interval between the last injection and the performance of OCTA. Last, our analysis was focused solely on evaluating the sources of newly developed NV during follow-up, without tracking the origins of preexisting NV. It is crucial that future research continues in this area to gain a more comprehensive understanding of the mechanisms behind NV development and to potentially uncover new insights into the variability of responses to NV treatment.

## Conclusions

WF-SS OCTA offers significant advantages for the long-term follow-up of DR and the observation of microvascular changes, such as IRMA and the development of NV. Changes in IRMA were closely related to the severity of retinal ischemia and treatment. Ongoing ischemic progression was a significant risk factor for vein-origin NVE. To highlight, our study confirmed the potential, yet relatively rare development of NV from IRMA in a large cohort, but the risk factors associated with this transformation require further exploration.

## *Acknowledgments*

**Declaration of Generative AI in Scientific Writing:** In December 2023, the authors used ChatGPT-4 for language optimization of the manuscript. After using this tool, the authors reviewed and edited the content as needed and took full responsibility for the content of the publication.

Disclosure: **X. Ding**, None; **F. Romano**, None; **I. Garg**, None; **J. Gan**, None; **K.M. Overbey**, None; **M.D. Garcia**, None; **F. Vingopoulos**, None; **Y. Cui**, None; **Y. Zhu**, None; **G. Baldwin**, None; **H. Choi**, None; **J.M. Rodriguez**, None; **M.J. Finn**, None; **P. Razavi**, None; **D.G. Vavvas**, Olix Pharma (C), Valitor (C), TwentyTwenty (C), Sumitomo/Sunovion (C), Cambridge Polymer Group (C), National Eye Institute (F), Research to Prevent Blindness (F), Loefflers Family Foundation (F), Yeatts Family Foundation (F), Alcon Research Institute (F); **D. Husain**, Allergan (C), Genentech (C), Omeicos Therapeutics (C), National Eye Institute (F), Lions Vision Gift (F), Commonwealth Grant (F), Lions International (F), Syneos LLC (F), the Macular Society (F); **D.M. Wu**, None; **N.A. Patel**, Alimera Sciences (C), Alcon (C), Allergan (C), Genentech (C), Eyepoint (C), Lifesciences Guidepoint (C), GLG (C); **L.A. Kim**, National Eye Institute (F), CureVac AG (F), Pykus Therapeutics (F); **J.W. Miller**, Heidelberg Engineering (C), Sunovion (C), KalVista Pharmaceuticals (C), ONL Therapeutics (C); National Eye Institute and Lowy Medical Research Institute (F); **J.B. Miller**, Alcon (C), Allergan (C), Carl Zeiss (C), Sunovion (C), Topcon (C), Genentech (C)

## *References*

1. Goldberg MF, Jampol LM. Knowledge of diabetic retinopathy before and 18 years after the Airlie House Symposium on Treatment of Diabetic Retinopathy. *Ophthalmology*. 1987;94(7):741–746.
2. Early Treatment Diabetic Retinopathy Study Research Group. Grading diabetic retinopathy from stereoscopic color fundus photographs–an extension of the modified Airlie House classification. ETDRS report number 10. *Ophthalmology*. 1991;98(5 suppl):786–806.
3. Early Treatment Diabetic Retinopathy Study design and baseline patient characteristics. ETDRS report number 7. *Ophthalmology*. 1991;98(5 suppl):741–756.
4. Early Treatment Diabetic Retinopathy Study Research Group. Fundus photographic risk factors for progression of diabetic retinopathy. ETDRS report number 12. *Ophthalmology*. 1991;98(5 suppl):823–833.
5. Wilkinson CP, Ferris FL, 3rd, Klein RE, et al. Proposed international clinical diabetic retinopathy and diabetic macular edema disease severity scales. *Ophthalmology*. 2003;110(9):1677–1682.
6. Lee CS, Lee AY, Baughman D, et al. The United Kingdom Diabetic Retinopathy Electronic Medical Record Users Group: report 3: baseline retinopathy and clinical features predict progression of diabetic retinopathy. *Am J Ophthalmol*. 2017;180:64–71.
7. Lee CS, Lee AY, Sim DA, et al. Reevaluating the definition of intraretinal microvascular abnormalities and neovascularization elsewhere in diabetic retinopathy using optical coherence tomography and fluorescein angiography. *Am J Ophthalmol*. 2015;159(1):101–110.e1.
8. Lains I, Wang JC, Cui Y, et al. Retinal applications of swept source optical coherence tomography (OCT) and optical coherence tomography angiography (OCTA). *Prog Retin Eye Res*. 2021;84:100951.
9. Ishibazawa A, Nagaoka T, Takahashi A, et al. Optical coherence tomography angiography in diabetic retinopathy: a prospective pilot study. *Am J Ophthalmol*. 2015;160(1):35–44.e1.
10. Fossataro F, Rispoli M, Pece A. OCTA in macular intraretinal microvascular abnormalities: retinal vascular density remodeling after panretinal photocoagulation. *Eur J Ophthalmol*. 2022;32(4):NP123–NP126.
11. Pan J, Chen D, Yang X, et al. Characteristics of neovascularization in early stages of proliferative diabetic retinopathy by optical coherence tomography angiography. *Am J Ophthalmol*. 2018;192:146–156.
12. Schaal KB, Munk MR, Wyssmueller I, Berger LE, Zinkernagel MS, Wolf S. Vascular abnormalities in diabetic retinopathy assessed with swept-source optical coherence tomography angiography widefield imaging. *Retina*. 2019;39(1):79–87.
13. Chua J, Sim R, Tan B, et al. Optical coherence tomography angiography in diabetes and diabetic retinopathy. *J Clin Med*. 2020;9(6):1723.
14. Sorour OA, Mehta N, Baumal CR, et al. Morphological changes in intraretinal microvascular abnormalities after anti-VEGF therapy visualized on optical coherence tomography angiography. *Eye Vis (Lond)*. 2020;7:29.
15. DaCosta J, Bhatia D, Crothers O, Talks J. Utilisation of optical coherence tomography and optical coherence tomography angiography to assess retinal neovascularisation in diabetic retinopathy. *Eye (Lond)*. 2022;36(4):827–834.
16. Memon AS, Memon NA, Mahar PS. Role of optical coherence tomography angiography to differentiate intraretinal microvascular abnormalities and retinal neovascularization in diabetic retinopathy. *Pak J Med Sci*. 2022;38(1):57–61.

17. Shimouchi A, Ishibazawa A, Ishiko S, et al. A proposed classification of intraretinal microvascular abnormalities in diabetic retinopathy following panretinal photocoagulation. *Invest Ophthalmol Vis Sci*. 2020;61(3):34.
18. Russell JF, Shi Y, Scott NL, Gregori G, Rosenfeld PJ. Longitudinal angiographic evidence that intraretinal microvascular abnormalities can evolve into neovascularization. *Ophthalmol Retina*. 2020;4(12):1146–1150.
19. Lu Y, Wang JC, Zeng R, et al. Quantitative comparison of microvascular metrics on three optical coherence tomography angiography devices in chorioretinal disease. *Clin Ophthalmol*. 2019;13:2063–2069.
20. Tsuboi K, Ishida Y, Wakabayashi T, Kamei M. Presumed glial sprouts as a predictor of preretinal neovascularization in retinal vein occlusion. *JAMA Ophthalmol*. 2022;140(3):284–285.
21. Garg I, Miller JB. Semi-automated algorithm using directional filter for the precise quantification of non-perfusion area on widefield swept-source optical coherence tomography angiograms. *Quant Imaging Med Surg*. 2023;13(6):3688–3702.
22. Ting DS, Cheung GC, Wong TY. Diabetic retinopathy: global prevalence, major risk factors, screening practices and public health challenges: a review. *Clin Exp Ophthalmol*. 2016;44(4):260–277.
23. Snodderly DM, Weinhaus RS, Choi JC. Neural-vascular relationships in central retina of macaque monkeys (Macaca fascicularis). *J Neurosci*. 1992;12(4):1169–1193.
24. Bresnick GH, Condit R, Syrjala S, Palta M, Groo A, Korth K. Abnormalities of the foveal avascular zone in diabetic retinopathy. *Arch Ophthalmol*. 1984;102(9):1286–1293.
25. Garg I, Uwakwe C, Le R, et al. Nonperfusion area and other vascular metrics by wider field swept-source OCT angiography as biomarkers of diabetic retinopathy severity. *Ophthalmol Sci*. 2022;2(2):100144.
26. Group UKPDS. Tight blood pressure control and risk of macrovascular and microvascular complications in type 2 diabetes: UKPDS 38. UK Prospective Diabetes Study Group. *BMJ*. 1998;317(7160):703–713.
27. Do DV, Han G, Abariga SA, Sleilati G, Vedula SS, Hawkins BS. Blood pressure control for diabetic retinopathy. *Cochrane Database Syst Rev*. 2023;3(3):CD006127.
28. Sauesund ES, Jorstad OK, Brunborg C, et al. A pilot study of implementing diabetic retinopathy screening in the Oslo region, Norway: baseline results. *Biomedicines*. 2023;11(4):1222.
29. Lu J, Hou X, Zhang L, et al. Association between body mass index and diabetic retinopathy in Chinese patients with type 2 diabetes. *Acta Diabetol*. 2015;52(4):701–708.
30. Kastelan S, Tomic M, Gverovic Antunica A, Ljubic S, Salopek Rabatic J, Karabatic M. Body mass index: a risk factor for retinopathy in type 2 diabetic patients. *Mediators Inflamm*. 2013;2013:436329.
31. Imesch PD, Bindley CD, Wallow IH. Clinicopathologic correlation of intraretinal microvascular abnormalities. *Retina*. 1997;17(4):321–329.
32. Ashton N. Arteriolar involvement in diabetic retinopathy. *Br J Ophthalmol*. 1953;37(5):282–292.
33. Shimizu K, Kobayashi Y, Muraoka K. Midperipheral fundus involvement in diabetic retinopathy. *Ophthalmology*. 1981;88(7):601–612.
34. Jacobs NA, Steele CA, Mills KB. Origin of disc new vessels assessed by videofluorography. *Br J Ophthalmol*. 1988;72(5):394–398.